

Article

Tryptophan Substitutions Reveal the Role of Nicotinic Acetylcholine Receptor α -TM3 Domain in Channel Gating: Differences between *Torpedo* and Muscle-Type AChR

Manuel Navedo, Madeline Nieves, Legier Rojas, and Jose A. Lasalde-Dominicci

Biochemistry, 2004, 43 (1), 78-84 • DOI: 10.1021/bi0356496

Downloaded from <http://pubs.acs.org> on December 10, 2008

More About This Article

Additional resources and features associated with this article are available within the HTML version:

- Supporting Information
- Access to high resolution figures
- Links to articles and content related to this article
- Copyright permission to reproduce figures and/or text from this article

[View the Full Text HTML](#)



ACS Publications
High quality. High impact.

Tryptophan Substitutions Reveal the Role of Nicotinic Acetylcholine Receptor α -TM3 Domain in Channel Gating: Differences between *Torpedo* and Muscle-Type AChR[†]

Manuel Navedo,[‡] Madeline Nieves,[‡] Legier Rojas,[§] and Jose A. Lasalde-Dominicci^{*‡}

Department of Biology, University of Puerto Rico, Rio Piedras, Puerto Rico 00931, and
Department of Physiology, Universidad Central del Caribe, Bayamón, Puerto Rico 00919

Received September 12, 2003; Revised Manuscript Received November 6, 2003

ABSTRACT: A recent tryptophan scanning of the α -TM3 domain of the *Torpedo californica* AChR demonstrated that this domain can modulate ion-channel gating [Guzman, G., Santiago, J., Ricardo, A., Martí-Arbona, R., Rojas, L., Lasalde-Dominicci, J. (2003) *Biochemistry* 42, 12243–12250]. Here we extend the study of the α -TM3 domain to the muscle-type AChR by examining functional consequences of single tryptophan substitutions at five conserved positions (α M282, α F284, α V285, α A287, and α I290) homologous to the α -TM3 positions that were recently characterized in the *Torpedo* AChR. Similarly to the *Torpedo* AChR, mutations α M282W and α V285W, which are presumed to face the interior of the protein, did not exhibit functional channel activity. Nevertheless, significant expression levels of these mutants were observed at the oocyte surface. In contrast to the *Torpedo* AChR, in the muscle-type AChR, tryptophan substitution at positions F284, A287, and I290 produces a significant increase in normalized macroscopic response. Single-channel recordings at low ACh concentration revealed that the increase in AChR sensitivity for the F284W, A287W, and I290W is due to an increase in the mean open duration. These results suggest that tryptophan substitution directly affects channel gating, primarily the channel closing rate. Our results suggest that residues facing the interior of the protein (i.e., α M282 and α V285) may similarly affect channel gating in *Torpedo* and muscle-type AChR. However, equivalent mutations (i.e., F284W and I290W) presumably facing the lipid environment display a very different functional response between these two AChR species.

The muscle-type acetylcholine receptor (AChR)¹ is a large allosteric membrane protein that mediates synaptic transmission at the vertebrate neuromuscular junction. AChRs are heteropentamers comprised of four different but highly homologous subunits designated as α , β , δ , and ϵ/γ (for reviews see refs 1–3). Each subunit contains an extracellular N-terminal domain (which include the ACh binding sites), four hydrophobic transmembrane (TM) domains (M1–M4), and a small extracellular C-terminal domain. Several studies have provided convincing evidence that the TM2 domain segments from each subunit cluster around a central axis to form the ion channel pore (4), and that the TM1 domain may partially contribute to channel formation in the open conformation of the receptor (5, 6). The TM3 and TM4 domains are thought to be located away from the channel pore in close proximity or exposed to the lipid interface.

It has been shown by our group and others that single amino acid perturbations at the postulated protein–lipid

interface, specifically within the TM4 domain, can dramatically alter the channel gating mechanism (7–14), suggesting that protein–lipid interactions play a role in AChR channel gating. The TM3 domain also has substantial contact with membrane lipids (15); however, its functional role and structural aspects have not yet been elucidated. We have used tryptophan mutagenesis to characterize the role of the γ -TM3 domain in the *Torpedo californica* AChR channel function (16). Single tryptophan substitutions at deduced lipid-exposed positions increased the macroscopic current of the AChR. In a recent study, we performed tryptophan scanning mutagenesis at 13 positions in the TM3 domain of the *Torpedo* AChR α -subunit (from residues M278 to I290; 17). Analysis of the periodicity of the functional response, as well as the normalized expression per volume change for each of these mutations, suggests that the α -TM3 domain of the *Torpedo* AChR is comprised of α -helical structures. Interestingly, in contrast to our previous studies of the α -TM4 domain (7–9, 13), tryptophan substitutions at lipid-exposed positions in the α -TM3 domain of the *Torpedo* AChR did not increase the normalized macroscopic current response.

Here we extend the study of the α -TM3 domain to the muscle-type AChR by examining functional consequences of single tryptophan substitutions at five conserved positions (α M282, α F284, α V285, α A287, and α I290) homologous to the α -TM3 positions that were recently characterized in

[†] This work was supported by NIH RO1GM56371 and GM08102–27 to J.L.D. M. Navedo and M. Nieves were supported by NIH-MBRS Research Initiative for Scientific Enhancement (5R25GM61151).

^{*} To whom correspondence should be addressed: Department of Biology, University of Puerto Rico, San Juan, PR 00931. Tel: 787–764–0000 ext. 2765. Fax: 787–753–3852. E-mail: joseal@coqui.net.

[‡] University of Puerto Rico.

[§] Universidad Central del Caribe.

¹ Abbreviations: AChR, nicotinic acetylcholine receptor; ACh, acetylcholine; TM, transmembrane domain.

the *Torpedo* AChR (17). Positions α F284 and α A287 of the *Torpedo* AChR have previously been shown to be in contact with the lipid interface (15). In this study, we found that tryptophan replacements at three positions within the α -TM3 domain (α F284, α A287, and α I290) affect gating. Meanwhile, tryptophan substitution of residues α M282 and α V285 suggests that these residues are critical for functional assembly of the muscle-type AChR. Residues α F284 and α V285 have been studied previously, and their role in channel gating is unequivocal (18, 19). De Rosa and colleagues demonstrated that position 8' of the TM3 segment of all subunits contribute independently and additively to the muscle-type AChR channel gating (18). Furthermore, a naturally occurring mutation within the α -TM3 domain (α V285I) was shown to be responsible for a form of congenital myasthenic syndrome (19). This work by Sine and colleagues demonstrated that the volume and stereochemistry of position α V285 were key components of the AChR channel gating mechanism. However, none of these previous studies used tryptophan substitutions at the indicated positions. Although the muscle-type and *Torpedo* AChRs α -subunits are 80% identical overall and 87% identical within the α -TM3 domains, tryptophan replacement at homologous positions displayed remarkable functional differences between these two AChR species, particularly at those sites that are located at presumed lipid-exposed positions. This study provides new insights regarding the role of the mammalian α -TM3 domain on AChR channel function.

MATERIALS AND METHODS

Mutations of the α -Subunit of Muscle-Type AChR. cDNAs encoding various subunits of the murine muscle-type AChR (pcDNA3- M β , M δ , and M ϵ) were kindly provided by Dr. A. Auerbach (New York State University, Buffalo, NY). The coding region of the α -subunit of the muscle-type AChR was subcloned into the EcoRI site of pGEM-11z(-) under control of the SP6 promoter (Promega, Madison, WI). Site-directed mutagenesis of the α -subunit of the muscle-type AChR was carried out by mismatch amplification using two sequential PCRs (20). The constructs were sequenced with Sequenase 2.0 (United States Biochemical Corp., Cleveland, OH) to confirm that the desired point mutation was present and that no additional mutations occurred within the α -subunit-coding region.

Expression in *Xenopus laevis* Oocytes. RNA transcripts were synthesized in vitro as described previously (7). Briefly, the RNA transcripts (10 ng/oocyte at a concentration of 0.2 μ g/ μ L) of α -, β -, δ -, and ϵ -subunits were injected into *Xenopus* oocytes at a 2:1:1:1 ratio.

Voltage Clamp Recordings. Three days after mRNA injection, ACh-induced currents were recorded by two-electrode voltage clamp with the Gene Clamp 500 amplifier (Axon Instruments, Union City, CA). The data were acquired using the program Whole Cell Program 2.3 (provided by Dr. J. Dempster). Impaled oocytes were perfused in the recording chamber at a rate of 15 mL/min with MOR-2 buffer [82 mM NaCl, 2.5 mM KCl, 5 mM MgCl₂, 1 mM Na₂HPO₄, 5 mM N-(2-Hydroxyethyl)piperazine-N'-2-ethanesulfonic acid (HEPES), and 0.2 mM CaCl₂ (pH 7.4)]. Acetylcholine was dissolved in the MOR-2 solution at the desired concentration. Electrodes were filled with 3 M KCl

and had resistances of less than 2 M Ω . All recordings were obtained at a holding potential of -70 mV. Dose-response data were collected and analyzed as described previously (11). Briefly, each dose-response curve was constructed from experiments in 5-12 oocytes per mutation. Data points for dose-response curves were taken from peak currents at six ACh concentrations (1, 3, 10, 30, 100, and 300 μ M). Dose-response curves were fitted with the equation $I/I_{\max} = 1/(1 + (EC_{50}/[\text{agonist}])^n)$ where I is the measured peak current, I_{\max} is the maximal response, n is the Hill slope, and EC_{50} is the concentration of agonist required for half-maximal response. The EC_{50} and Hill coefficient values for individual oocytes were averaged to generate final estimates. An unpaired t-test for unequal variance was used for statistical comparisons between two data sets (Prism). Data are given as mean \pm SD.

[¹²⁵I]- α -Bungarotoxin Binding Assay. The expression of the AChR in oocyte membranes was determined by assaying the binding of [¹²⁵I]- α -bungarotoxin ([¹²⁵I]- α BTX) (Amersham Life Sciences, Arlington Heights, IL) to intact oocytes, as described previously (11).

Normalized Macroscopic AChR Response. To determine the normalized functional response to ACh, the [¹²⁵I]- α -bungarotoxin binding assay was performed immediately following voltage clamping. The protocol to normalize the ACh-induced response is to apply a single ACh concentration of 300 μ M per oocyte and then normalize the amount of current measured to the toxin binding sites in the oocyte surface (nA/fmol). This ACh concentration was selected based on the dose-response curve of the wild-type AChR. This is defined as the peak of the ACh-induced current (nA) per fmol of surface α -bungarotoxin binding sites. Using this approach, we can determine the normalized channel response to ACh.

Patch Clamp Recordings. *Xenopus* oocytes were placed in a recording chamber containing a bath solution of 100 mM KCl, 1 mM MgCl₂, and 10 mM HEPES (pH 7.2) at 20-22 °C. The patch pipets were made of thick-walled borosilicate glass (Sutter Instruments, Novato, CA). Pipets typically had resistance of 2-4 M Ω . The pipet solution contained 100 mM KCl, 10 mM HEPES, 10 mM EGTA (pH 7.2), and 4 or 100 μ M ACh. All experiments were performed in the cell-attached configuration at a membrane potential of -100 mV (21). Single-channel currents were recorded using an Axopatch 200B patch clamp amplifier (Axon Instruments), filtered at 5 kHz and stored on VHS tapes using a digital data recorder (VR-10B, Instrutech Corp., Mineola, NY). The data traces were played back into a Pentium III-based computer through a DigiData 1200 interface (Axon Instruments) and digitalized at 50 kHz using the program Fetchex (Axon Instruments). Single-channel events at low ACh concentration (4 μ M) were detected with a half-amplitude crossing algorithm (pClamp6). Open and closed time duration distributions were constructed from pClamp6-generated files using a logarithmic abscissa and a squared root ordinate (22) and fitted using the maximum likelihood algorithm with the appropriate number of components using the program pSTAT (Axon Instruments). At 100 μ M ACh concentration, all the channels in the pipet are desensitized. However, individual receptors randomly revert to the nondesensitized state, and the kinetic of the open and closing states of only one channel can be measure as a burst

		282 284 287 290
Mouse	PLIGKYMLFT	MVFVIASI IITVIVINT
Torpedo	PLIGKYMLFT	MIFVISSI IITVVVINT
Human	PLIGKYMLFT	MVFVIASI IITVIVINT
Xenopus	PLIGKYMLFT	MVFVIASI IITVIVINT
Rat α 2	PLIGEYLLFT	MIFVLSI VITVFLNV
Rat α 3	PLIGEYLLFT	MIFVLSI VITVFLNV
Rat α 4	PLIGEYLLFT	MIFVLSI VITVFLNY
Rat α 5	PLIGEYLVFT	MIFVLSI MVTVFAINI
Rat α 6	PLVGEYLLFT	MIFVLSI VVTVFLNI
Rat α 7	PLIAQYFAST	MIIVGLS VVTVIVLRY
		6' 8'9' 11' 14'

FIGURE 1: Sequence alignment of the TM3 domain of α -subunits from various species. Residues shown in bold were mutated to tryptophan. Note the high degree of conservation at the position studied (282–290). Prime number nomenclature was located at the bottom of the alignment sequence.

of activity. A burst of openings corresponding to a single channel were defined as a series of openings separated by closed intervals greater than some critical duration (τ_{crit}); this duration was taken as the point of intersection of the predominant closed component and the succeeding one in the closed time histogram, as described elsewhere (12, 23). Single-channel events at 100 μ M ACh concentration were detected and idealized with a half-amplitude crossing criterion using the program QUB (QUB suite, State University of New York, Buffalo). Only bursts that exhibited durations longer than 100 ms and more than 10 openings per burst were used for further analysis. The resulting open and closed time intervals from single patches at 100 μ M ACh were analyzed according to a kinetic scheme using the program MIL (QUB suite, State University of New York, Buffalo). The dead time used was set to 30 μ s. Probability density functions of open and closed durations were calculated from the fitted rate constants and superimposed on the experimental dwell-time histograms (24).

RESULTS

Tryptophan was introduced at five residues (M282, F284, V285, A287, and I290; see Figure 1) located near the center of the TM3 domain of the muscle-type AChR α -subunit. Positions α F284 and α V285 have been previously studied (18, 19); however, none of the previous studies made tryptophan substitutions at these positions. *Xenopus* oocytes were injected with either wild type or a mutant α -subunit, along with wild-type β -, δ -, and ϵ -subunits. Figure 1 shows aligned primary sequences of α -TM3 domain from five species, including six neuronal AChR α -subunits. Residues 282, 284, and 285 are completely conserved among the α -TM3 domain, and residues 287 and 290 are highly conserved within the same segment. This pattern of conservation suggests that these positions may be important for proper channel function. Among the residues mutated, residues F284 and A287 were suggested to be in contact with the lipid interface in the *Torpedo* AChR (15).

Expression of Mutant AChRs. To determine the expression level of each AChR studied, [125 I] α -BTX binding assays were performed on *Xenopus* oocytes expressing wild-type or mutant AChRs. All the mutants displayed expression levels similar to that of the wild-type AChR, except for α V285W, which was expressed at lower levels, as compared to wild type (Table 1). These results suggest that the TM3 domain

Table 1: Functional Consequences of α -TM3 Trp Mutations^a

AChR type ($\alpha\beta\delta\epsilon$)	expression level (fmol)	EC ₅₀ (μ M)	Hill coefficient	normalized response (–nA/fmol)
wild type	2.3 \pm 0.5	54 \pm 1	1.4 \pm 0.5	722 \pm 265
M282W	1.7 \pm 0.7 [†]	ND	ND	ND
F284W	1.4 \pm 0.3 [†]	12 \pm 2	1.0 \pm 0.6	1284 \pm 536 [†]
V285W	0.9 \pm 0.5	ND	ND	ND
A287W	2.1 \pm 1	42 \pm 1*	1.4 \pm 0.6	1173 \pm 490 [†]
I290W	2.4 \pm 0.3	18 \pm 1*	1.4 \pm 0.6	1715 \pm 276 [†]

^a Values are given as the mean \pm the standard deviation. Normalized peak channel activity for individual oocytes was obtained by dividing the ACh-induced current at 300 μ M by the fmol of AChR expressed on each oocyte. Hill coefficients and normalized responses were calculated using 4–13 oocytes. ND, no detectable current. * $P < 0.001$. [†] $P < 0.005$.

tolerates aromatic side chain substitutions at all positions tested.

Functional Consequences of Mutant AChRs. To determine the functional effect of these mutations on channel activity, mutant AChRs were evaluated with a two-electrode voltage clamp following the application of 300 μ M ACh. This experiment was designed to determine if all mutant AChRs assemble into functional channels. Ionic currents elicited by ACh application were normalized to the corresponding receptor expression level in femtomoles (Table 1). Of all the mutations, only two, α M282W and α V285W, failed to display ACh-induced currents at all the tested concentrations. This loss of function suggests that tryptophan side chain substitutions at positions α M282 and α V285 alter the conformational changes required either for correct channel assembly or for ion channel function. Tryptophan substitutions at residues α F284, α A287, and α I290 produced current amplitudes ranging from 1200 to 1800 nA/fmol (Table 1), suggesting that this position can accommodate aromatic side chain substitutions and still produce functional channels.

To further characterize the functional properties of mutant AChRs, dose–response curves were constructed for wild type and each of the functional mutant receptors (α F284W, α A287W, and α I290W). Figure 2B shows a representative family of currents for the wild-type and functional mutant AChRs. All functional mutant AChRs exhibited statistically significant reductions in EC₅₀ values (Figure 2A, Table 1). The α F284W and α I290W mutations showed EC₅₀ values 4.5- and 3-fold lower than wild-type levels, respectively. The α A287W mutant exhibited a slightly, but significant, decrease in EC₅₀ value, although its normalized response was very similar to the other functional mutant AChRs. There were no significant changes in the Hill coefficient for the functional mutant AChRs, indicating that each mutation changed the ACh EC₅₀ value without changing the cooperativity.

Single-Channel Data. We used the patch clamp technique (21) to gain insight into the results obtained at the macroscopic level and to further examine the single-channel properties of wild-type and functional mutant AChRs. Figure 3 shows single-channel traces and open time histograms for wild-type and functional mutant AChRs at a low ACh concentration (4 μ M). α F284W and α I290W showed the longest mean open times, which were 5.4- and 2.3-fold higher than wild type, respectively. The mean open time of α A287W was slightly larger than wild type (Table 2). No significant changes in conductance were observed for any

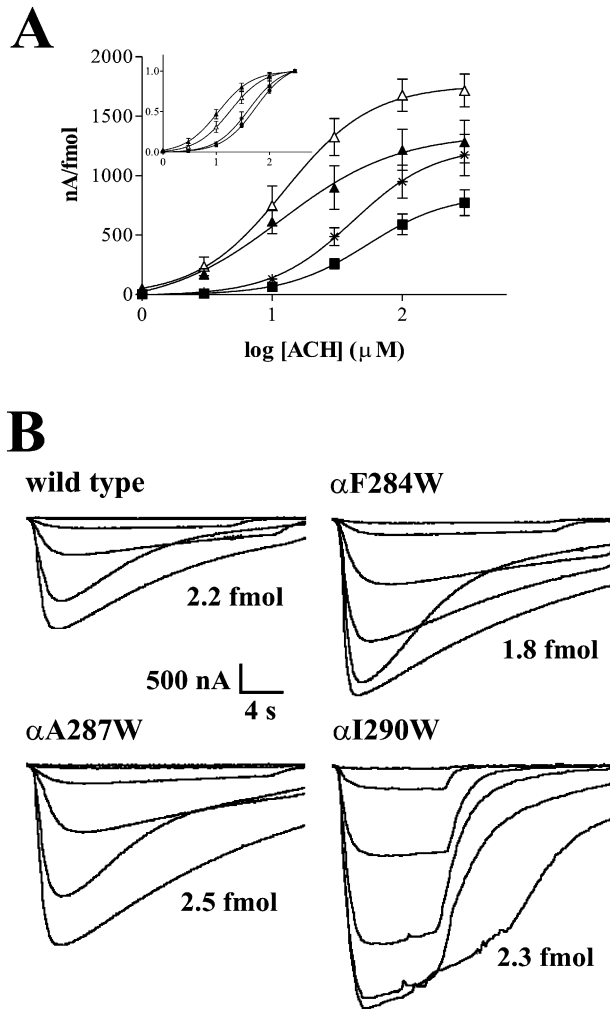


FIGURE 2: Functional effects of tryptophan mutations within α -TM3. (A) ACh dose-response curves were determined in *Xenopus laevis* oocytes expressing wild type (black squares), α F284W (black triangles), α A287W (asterisks), and α I290W (open triangles) AChRs. Data are expressed as ACh-induced currents (nA) per fmol of surface α -BTX binding sites. Dose-response data was collected from peak currents at six ACh concentrations (1–300 μ M). Each dose-response curve was normalized to maximal current of each oocyte tested. Data for each ACh concentration are expressed as mean \pm SE of 6–12 individually tested oocytes. (B) Families of ACh-induced macroscopic currents derived from individual oocytes from wild type and α F284W, α A287W, and α I290W AChRs were recorded by two-electrode voltage clamp, as indicated. The macroscopic current response of each oocyte was normalized to the surface α -BTX binding for each individual oocyte. Surface AChRs expression levels (fmol) for each oocyte is included alongside each family of currents. Inset figure in panel A represents dose-response curves for each of the AChRs tested normalized to maximal response.

of the functional mutations at a holding potential of -100 mV, as compared to wild-type AChRs.

We next activated wild-type and functional mutant AChRs with a high concentration of ACh (100 μ M). This concentration produces a clear cluster of events corresponding to a single channel (25), as illustrated in Figure 4. The closed-time distribution was well fitted by the sum of three to four components, for all the AChRs tested. The most abundant component corresponds to closing events within the burst. The mean open time in α F284W was 8.4-fold higher as compared to wild type, whereas mutations α A287W and α I290W increase the mean open time by 1.3- and 1.7-fold,

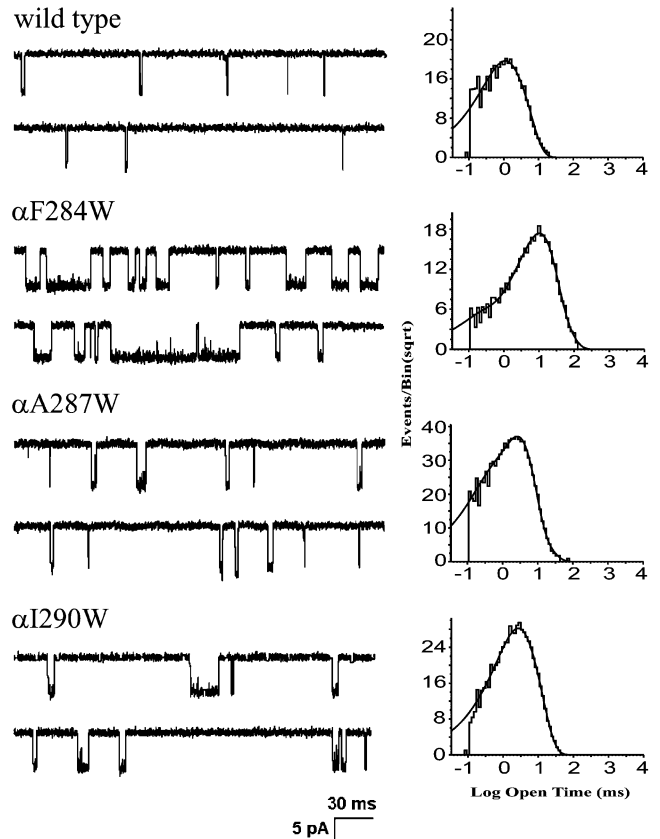
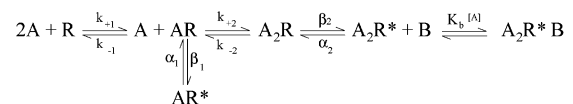


FIGURE 3: Single channel currents for wild type and α F284W, α A287W, and α I290W mutant AChRs at low ACh concentrations. Single-channel currents, elicited by 4 μ M ACh, were recorded from *Xenopus* oocytes expressing either wild type or various mutant muscle-type AChRs, as indicated. Right panel, open duration time histograms corresponding to the various AChRs studied was fitted with exponential functions of the appropriate number of components using the maximum likelihood algorithm. The data were filtered at 5 kHz for each current sample displayed and channel openings are shown as upward deflections (left panel). All channels were recorded at a holding potential of -100 mV, a sampling rate at 50 kHz and at a temperature of 22 $^{\circ}$ C.

respectively (Table 3). In addition, α F284W and α I290W showed 2.3- and 2.5-fold increases in the mean burst duration, respectively, as compared to wild type (Table 3). The increase in mean burst duration for the α F284W and α I290W is consistent with the increase in the macroscopic current observed for each mutation. Because each burst of activity reflects the activity of a single AChR at 100 μ M ACh, open and closed time data can be used for kinetic analysis. To interpret the kinetic behavior of these mutations, we used a simple kinetic model with two open states:



In this scheme, R is the receptor, A is ACh, A_2R is the biliganded species, and AR^* and A_2R^* are the monoliganded and biliganded (and most abundant) open-states of the receptor-ligand complex, respectively. k_{+1} and k_{+2} are the binding rate constants, and k_{-1} and k_{-2} are the first and second dissociation rate constants for the first and second sites, respectively. α_1 and α_2 are the fast and slow closing rate constants, respectively, and β_1 and β_2 are the fast and

Table 2: Single-Channel Parameters at Low ACh Concentration^a

AChR	[ACh] (μM)	patches/events ^b	τ_{o1} (ms)	fraction	τ_{o2} (ms)	fraction	rate ($1/\tau_o$)	
							α_1 (s^{-1})	α_2 (s^{-1})
wt	4	3/6996	0.656	0.407	1.64	0.593	1524	610
αF284W	4	3/5024	18.4	0.128	8.90	0.826	54	112
αA287W	4	8/25894	0.301	0.152	2.38	0.804	3322	421
αI290W	4	8/14670	1.73	0.426	3.79	0.574	578	264

^a Single-channel data were recorded in cell-attached patches at a holding potential of -100 mV, 5 kHz, and 22 °C. The sampling rate was set at 50 kHz for data acquisition. ^b Number of patches/number of events.

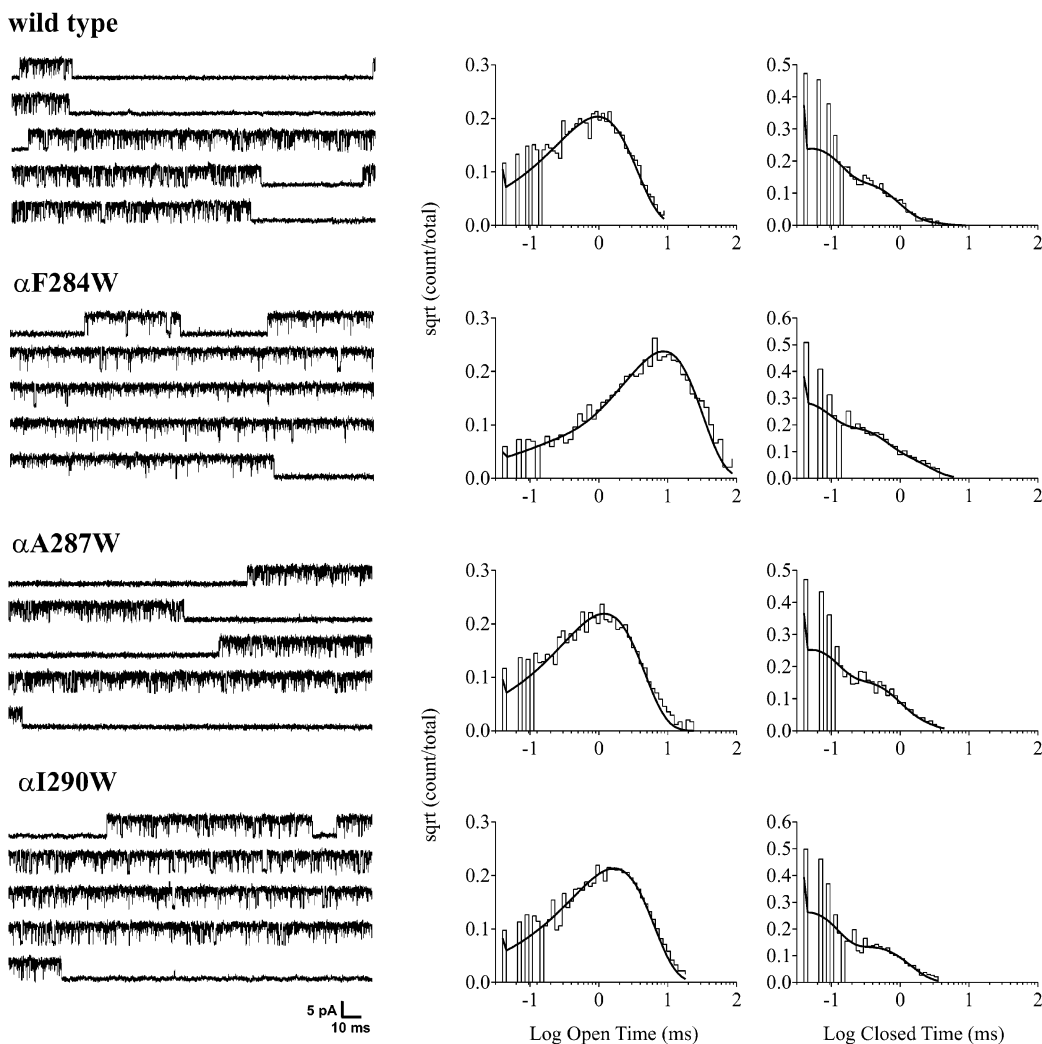


FIGURE 4: Single channel currents for wild type and αF284W , αA287W , and αI290W at high ACh concentrations. Single-channel currents elicited by $100 \mu\text{M}$ ACh, recorded from *Xenopus* oocytes expressing AChRs containing wild-type muscle-type and tryptophan-substituted mutant AChRs; αF284W , αA287W , and αI290W . Right side, open and closed duration time histograms corresponding to the specific AChR studied fitted with exponential functions of the appropriate number of components using the maximum likelihood algorithm. The data were filtered at 5 kHz for each current sample displayed and channel openings shown as upward deflections (left side panel). Each current trace represents continuous single-channel recordings corresponding to bursts of activity for each of the AChRs tested. Note the increase in burst duration for the αF284W and αI290W mutants as compared to wild type and the αA287W mutant. All channels were recorded at a holding potential of -100 mV, sampling rate at 50 kHz and at a temperature of 22 °C.

slow open rate constants, respectively. A_2R^*B represents the biliganded open-state of the receptor blocked by the agonist. K_b [A] is the equilibrium constant of the channel block state by the agonist. We evaluated the effective opening rate at $100 \mu\text{M}$ ACh associated with isomerization of the channel to the two open-channel states AR^* and A_2R^* .

At high ACh concentration ($100 \mu\text{M}$), the αF284W mutant showed the largest increase in open duration, from 0.95 in the wild type to 8 ms (see Table 3), even though the relative

difference in volume between phenylalanine and tryptophan is smaller compared to the other tryptophan substitutions that were made (27). A burst oriented analysis demonstrates that this increase in open channel probability is the result of an increase in the effective opening rate (25480 s^{-1}) combined with a 4.6-fold decrease in the closing rate (397 s^{-1}). The combined alteration in the channel gating of the αF284W leads to the largest biliganded equilibrium constant ($\Theta_2 = 64$) among these three mutants (Table 3). Although the burst

Table 3: Single-Channel Parameters at 100 μ M [ACh] for α -TM3 Trp Mutations^a

AChR	events	bursts	τ_o (ms)	f	τ_c (ms)	f	k_{-2}	β_2	α_2	Θ_2	K_b^c	τ_B (ms) ^d
wt	19941	42	0.95	0.94	0.045	0.63	3473	19002	1818	10	1.4	49.1
α F284W	14291	121	8.0	0.97	0.033	0.62	4221	25480	397	64	78	115
α A287W	27141	66	1.2	0.95	0.041	0.57	4462	19472	1491	13	2.0	58.3
α I290W	45261	155	1.6	0.96	0.040	0.65	3760	21188	1132	18	55	123

^a Single channel data were recorded in cell-attached patches at a holding potential of -100 mV, 5 kHz, and 22 °C. The sampling rate was set at 50 kHz for data acquisition. ^b Θ_2 is the diliganded channel open equilibrium constant. This constant corresponded to ratios of opening and closing di-liganded rate constants. Values are results of fit scheme 1 to the data obtained at 100 μ M ACh. ^c K_b is the equilibrium constant of the channel block state by the agonist in units of mM. ^d τ_B is the mean burst duration.

duration of the α F284W increases 2-fold as compared to the wild type, estimation of microscopic rate constant using a model-dependent analysis (24) shows that this mutant displayed a profound agonist-induced block (see Table 3). This agonist-induced block could be responsible for the reduced macroscopic response of the α F284W compared to the α I290W mutation shown in Figure 2A. The α I290W mutant displayed a modest increase in the effective opening rate (21188 s⁻¹) combined with a significant decrease in the closing rate (1132 s⁻¹) and the longest burst durations (123 ms) among these three mutants. The α A287W mutant produced a modest decrease in the closing rate (1491 s⁻¹), and the effective opening rate was unaffected.

DISCUSSION

In this study, we extended the used of tryptophan mutagenesis at five residues (α M282, α F284, α V285, α A287, and α I290) presumed to be located near the center of the α -TM3 domain to delineate structural and functional properties of the muscle-type AChR. The selection of these five residues was based on a previous study in which we evaluate the secondary structure and the spatial organization of the *T. californica* α -TM3 domain (17). In the aforementioned study, tryptophan replacement at these five residues produce the most dramatic effects in AChR channel function and assembly. Two of the studied residues (α F284 and α A287) were labeled in the *Torpedo* AChR with hydrophobic probes and were proposed to be exposed to the protein–lipid interface (15). The same study detected no such labeling at positions α M282, α V285, or α I290. If we assume the same α -helical structure (17) for the muscle-type α -TM3 domain, positions α M282 and α V285 would be predicted to face the interior of the protein, whereas position α I290 could have a partial exposure to the lipid interface (Figure 5). Thus, the lack of functional response in α M282W and α V285W in both *T. californica* (17) and muscle-type AChR suggests that an increase in volume at these two positions of the α -TM3 domain can impair the channel gating mechanism in both receptor types. This loss in functional response could be due to an increase in the steric forces between transmembrane segments, or to a defect in the assembly of the AChR caused by a disruption of helix–helix interactions. It was well established by Sine’s group that the volume of the side chain at the α V285 position is critical for proper channel function, and that changes in side chain volume at this site affect channel closing and opening (19). On the basis of these previous results, it was expected that substitution of tryptophan for valine at position α V285 could diminish or even abolish channel function. It remains to be established whether the α M282 position has the same physical and chemical requirements as that of the α V285 position for proper channel gating.

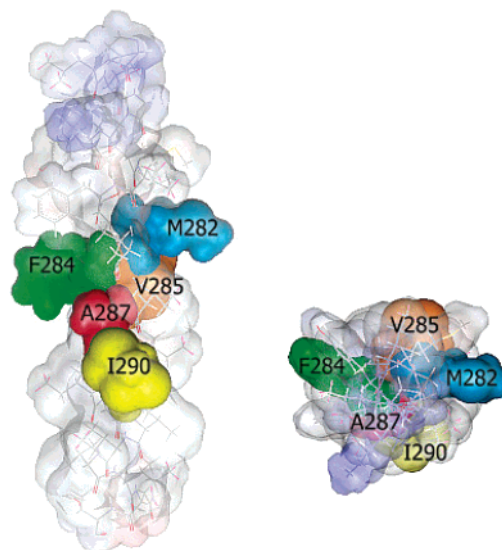


FIGURE 5: Molecular model of the α -TM3 domain of the AChR. The helical structure of muscle-type α -TM3 segment was modeled using Biomer V1.0 alpha (see <http://www.scripps.edu/n~nwhite/B>). An α -helical structure for the α -TM3 was minimized using the Fletcher-Reeves conjugated gradient algorithm (<2000 iterations), as described in ref 17. Minimized structures for wild type shows lipid exposed positions from a side and top views. Positions F284 and A287, which have been previously shown to be exposed to the membrane lipids, are oriented to the left side of the putative helix, while residues M282 and V285 are facing other transmembrane domains deep within the interior of the protein. This helical model predicts that position I290 is less embedded in the interior of the protein, possibly facing a neighboring transmembrane segment from the same subunit or of other subunit.

Our results from ACh-induced macroscopic currents suggest that positions α F284, α A287, and α I290 can tolerate hydrophobic aromatic side chain substitutions and play an important role in channel gating of the muscle-type AChR. The present study contrasts with recent results in the α -TM3 domain *Torpedo* AChR; tryptophan substitution at the same three positions did not produce such an increase in the normalized macroscopic response (17). Moreover, the normalized macroscopic response for the equivalent mutations in the *Torpedo* was lower or similar as the wild type and the EC₅₀ was only reduced for the F284W mutation. Therefore, this study raises the question of how identical structural alteration at homologous residues that are presumably exposed to the lipid environment can modulate channel gating in such a remarkably different manner in these two AChR species. The differences between α -TM3 mutations in the muscle-type and *Torpedo* AChR could be because (i) the muscle-type AChR contains the ϵ -subunit, whereas the *Torpedo* AChR contains the γ -subunit; however, the presence of the ϵ -subunit does not alter the functional pattern of

residues facing the interior of the protein (i.e., α M282 and α V285), (ii) minor differences in the primary structure that can alter secondary structure and/or localized helix orientations that could lead to different helix–helix interactions of the α -TM3 domain between the two species, or (iii) different degrees of orientation of these domains to the lipid environment that could produce different patterns of lipid–protein interactions between these two species. A recent AChR structure proposed for *T. marmorata* places residues α A287 and α I290 facing the lipid–protein interface and residue α F284 appears to be buried between the TM1 and TM2 domains (26). These findings suggest that α F284 modulation of channel gating is either via allosteric interactions between TM1 and TM2 domains, or due to different α F284 orientations in the lipid interface of muscle-type or *Torpedo* AChR which, in turn, result in different alterations of channel gating. The possible mechanisms responsible for the observed differences between mutations in the α -TM3 domain of muscle type and *Torpedo* AChRs remain to be determined.

The present kinetic analysis suggests that tryptophan substitutions at positions α F284, α A287, and α I290 differentially affect channel gating. At a low ACh concentration (4 μ M), the α F284W, α A287W, and α I290W mutants primarily affect gating by reducing the channel closing rate (Table 2). The single channel data analysis at a 100 μ M ACh demonstrated that the functional response of these three mutations is very different (Table 3). The α F284W mutation not only reduces the closing rate, but also increases the effective opening rate and displayed a strong agonist-induced block. This channel block is consistent with the reduction in the macroscopic current response of this mutation compared to the α I290W mutation (Figure 2). These differences in the functional responses of these three mutants could be due to distinct physical requirements and dynamics of channel gating in the environment around these individual α -TM3 positions. Overall, the single channel data analysis matched the data obtained from normalized macroscopic currents for these three gain-in-function mutations.

From the results of a mutagenesis analysis, De Rosa and colleagues (18) proposed that only hydrophobic nonaromatic amino acids at position α F284 increase the mean open duration. They based their conclusions on the fact that substitution of phenylalanine for tyrosine at position α F284 did not significantly alter the kinetic properties of the channel. In this work, tryptophan substitution at the aforementioned position revealed a 5.4-fold increase in the mean open duration, as compared to wild type. The increase in open duration is more dramatic than the one induced by isoleucine substitution at the same position, as reported by De Rosa and colleagues (18), or even our previous tryptophan substitution at the lipid-exposed position C418 in the α -TM4 segment (11). Tyrosine has 14% less volume than tryptophan, while its volume is very similar to that of phenylalanine (27). Furthermore, the hydroxyl group of tyrosine allows polar interactions. Thus, the kinetic differences that are observed between the α F284Y AChR mutant (18) and our α F284W mutant could be due to polar interactions that mediate the wild-type-like activity in α F284Y AChRs, rather than the volume of the side chain itself. A tryptophan substitution at position α F284 or positions α A287 and α I290 could better penetrate the membrane lipid interface, thereby forming van der Waals or dipole interactions that stabilize the open state

of the AChR. Another possibility is that the natural aromaticity of tryptophan gives rise to favorable interactions with the membrane complex to stabilize the open channel state. It has been shown that the flat rigid shape of tryptophan and its π -electron cloud favors the localization of this amino acid in the membrane interface environment (28). We observed similar effects at the α G421 position, when phenylalanine and tryptophan substitution dramatically affected channel function, but tyrosine substitution led to wild-type-like AChR activity at the single-channel level (8). In summary, the present study provides additional evidence supporting the role of the α -TM3 domain in channel gating and the functional role of lipid-exposed domains in the differential modulation of ion channel function in different AChR species.

REFERENCES

- Karlin, A., and Akabas, M. H. (1995) *Neuron* 15, 1231–1244.
- Changeux, J. P., and Edelman, S. J. (1998) *Neuron* 21, 959–980.
- Karlin, A. (2002) *Nat. Rev. Neurosci.* 3, 102–114.
- Unwin, N. (1995) *Nature* 373, 37–43.
- Akabas, M. H., and Karlin, A. (1995) *Biochemistry* 34, 12496–12500.
- Zhang, H., and Karlin, A. (1997) *Biochemistry* 36, 15856–15864.
- Lee, Y. H., Li, L., Lasalde, J., Rojas, L., McNamee, M., Ortiz-Miranda, S. I., and Pappone, P. (1994) *Biophys. J.* 66, 646–653.
- Lasalde, J. A., Tamamizu, S., Butler, D. H., Vibat, C. R., Hung, B., and McNamee, M. G. (1996) *Biochemistry* 35, 14139–14148.
- Ortiz-Miranda, S. I., Lasalde, J. A., Pappone, P. A., and McNamee, M. G. (1997) *J. Membr. Biol.* 158, 17–30.
- Bouzat, C., Roccamo, A. M., Garbus, I., and Barrantes, F. J. (1998) *Mol. Pharmacol.* 54, 146–153.
- Tamamizu, S., Lee, Y., Hung, B., McNamee, M. G., and Lasalde-Dominicci, J. A. (1999) *J. Membr. Biol.* 170, 157–164.
- Bouzat, C., Barrantes, F., and Sine, S. (2000) *J. Gen. Physiol.* 115, 663–672.
- Tamamizu, S., Guzman, G. R., Santiago, J., Rojas, L. V., McNamee, M. G., and Lasalde-Dominicci, J. A. (2000) *Biochemistry* 39, 4666–4673.
- Bouzat, C., Gumilar, F., del Carmen Esandi, M., and Sine, S. M. (2002) *Biophys. J.* 82, 1920–1929.
- Blanton, M. P., and Cohen, J. B. (1994) *Biochemistry* 33, 2859–2872.
- Cruz-Martin, A., Mercado, J. L., Rojas, L. V., McNamee, M. G., and Lasalde-Dominicci, J. A. (2001) *J. Membr. Biol.* 183, 61–70.
- Guzman, G. R., Santiago, J., Ricardo, A., Marti-Arbona, R., Rojas, L., and Lasalde-Dominicci, J. A. (2003) *Biochemistry* 42, 12243–12250.
- De Rosa, M. J., Rayes, D., Spitzmaul, G., and Bouzat, C. (2002) *Mol. Pharmacol.* 62, 406–414.
- Wang, H. L., Milone, M., Ohno, K., Shen, X. M., Tsujino, A., Batocchi, A. P., Tonali, P., Brengman, J., Engel, A. G., and Sine, S. M. (1999) *Nat. Neurosci.* 2, 226–233.
- Ho, S. N., Hunt, H. D., Horton, R. M., Pullen, J. K., and Pease, L. R. (1989) *Gene* 77, 51–59.
- Hamill, O. P., Marty, A., Neher, E., Sakmann, B., and Sigworth, F. J. (1981) *Pflugers Arch.* 391, 85–100.
- Sigworth, F. J., and Sine, S. M. (1987) *Biophys. J.* 52, 1047–1054.
- Wang, H. L., Auerbach, A., Bren, N., Ohno, K., Engel, A. G., and Sine, S. M. (1997) *J. Gen. Physiol.* 109, 757–766.
- Qin, F., Auerbach, A., and Sachs, F. (1996) *Biophys. J.* 70, 264–280.
- Sakmann, B., Patlak, J., and Neher, E. (1980) *Nature* 286, 71–73.
- Miyazawa, A., Fujiyoshi, Y., and Unwin, N. (2003) *Nature* 424, 949–955.
- Chothia, C. (1975) *Nature* 254, 304–308.
- Yau, W. M., Wimley, W. C., Gawrisch, K., and White, S. H. (1998) *Biochemistry* 37, 14713–14718.